8th International Conference on Water Resources and Arid Environments (ICWRAE 8): 282-298
22-24 January 2019*, Riyadh, Saudi Arabia*

Electrospun Poly (Vinyl Alcohol)/ Poly Ethylene Glycol/ Molybdenum Trioxide Nanofibers Composite for Highly Efficient Adsorptive Water Treatment Applications

[1]M.R. El-Aassar, [2]Mohamed Elnouby, [3]Fatima Hafez Kamal, [3]Nagwa Abdel Fatah Badawy and [3]Shimaa I. Amer

[1]Polymer Materials Research Department,
Advanced Technology and New Material Research Institute, City of Scientific Research and Technological Applications (SRTA-City), New Borg El-Arab City 21934, Alexandria, Egypt
[2]Composites and Nanostructured Materials Research Department,
Advanced Technology and New Material Research Institute, City of Scientific Research and Technological Applications (SRTA-City), New Borg El-Arab City 21934, Alexandria, Egypt
[3]Department of Chemistry, Faculty of Science, Al-Azhar University, Cairo, Egypt

Abstract: In this work, Poly (vinyl alcohol) (PVA)/ poly ethylene glycol (PEG) have been fabricated by electrospinning and chemically crosslinked using glutaraldehyde (GA) with different concentration to improve the water resistance of nanofibers. The effects of the different concentration of GA on the solution properties of PVA/PEG/GA blends and on the morphology of the resultant nanofibers were studied. The surface morphology and the average diameter of the blend nanofibers are dependent on initially added GA concentrations. The effects of the GA on swelling properties and mechanical properties of the crosslinked PVA/PEG nanofibers were examined. PVA/PEG/GA blends composite nanofibers were modulated by introducing molybdenum trioxide nanoparticles (MoO_3) nanoparticles and explored for sustainable contaminant removal. The PVA/PEG/GA-MoO_3 composite nanofibers were characterized using scanning electron microscopy (SEM), fourier transform infrared spectroscopy (FTIR), thermogravimetric analysis (TGA) and swelling properties, respectively. PVA/PEG/GA-MoO_3 composite nanofibers were estimated by determining methylene blue (MB) adsorption capacity and the composite nanofibers exhibited excellent adsorption capacity of MB from aqueous synthetic samples. The effects of experimental parameters, including initial MB concentration, contact time, adsorbent doses, solution pH, temperature and NaCl concentration, on the removal of MB were determined in a batch system to optimize the adsorption conditions. The adsorption process of MB could be described by adsorption isotherm models, thermodynamic study and kinetic study in batch experiments. The results demonstrate that these nanofibers could be useful in the field of water remediation.

Key words: Electrospinning · PVA · Adsorption · Nanocomposites · Water treatment

INTRODUCTION

In current years, Organic dyes and pigments are common water pollutants, which are frequently found in many industries effluents such as textile finishing, cosmetics, leather, printing and paper [1]. Water that has been contaminated by dyes poses a tremendous threat to ecological and human health, since most of these dyes are not degradable because they resist aerobic digestion and are stable to heat, light and oxidizing agents [2]. The dyes are one of the most hazardous chemical compound classes found in textile industrial waste water. These can be easily observed even at low concentration make water highly detrimental, which leads the harmful to the environment and human health such as allergy, skin irritation, dermatitis and also provoke cancer and mutation in humans [3, 4]. Methylene blue (MB), a common pollutant in dye effluents, is difficult to remove completely

Corresponding Author: M.R. El-Aassar, Polymer Materials Research Department, Advanced Technology and New Material Research Institute, City of Scientific Research and Technological Applications (SRTA-City), New Borg El-Arab City 21934, Alexandria, Egypt E-mail: mohamed_elaassar@yahoo.com.

and resistant to biodegradation because of its stable aromatic structure consisting of a chromophore and polar groups, it can cause heart rate increasing, nausea and vomiting [5]. Various techniques such as coagulation, precipitation, membranes separation process, ion exchange, reverse osmosis and biodegradation have been recently developed for removal of dyes from waste water. These techniques are time-consuming and involve high operation costs. However, adsorption technique has attracted extensive research interest due to its high efficiency, low cost and providing the simplicity in operation and flexibility [6]. Recently, the development of nonmaterials suggests that many of the current water-treatment problems might be resolved or greatly ameliorated by using various nanostructures. Recently, the development of nonmaterials suggests that many of the current water-treatment problems might be resolved or greatly ameliorated by using various nanostructures. Polymeric nanofibers has been used as an absorbent to purify water for its unique properties and used in many applications such as filtration, material reinforcements, insulation and energy storage [7]. Numerous techniques, such as phase separation [8], drawing [9], template synthesis [10] and electrospinning [11], have been adapted to synthesis polymeric nanofibers. Among these techniques, electrospinning is a process carried out at room temperature that allows the production of polymer fibers with diameters in the sub-micron size range, through the application of an external electric field, keeping intact the bulk properties of the polymers. Electrospun membranes possess some unique structural features, such as a high surface to volume ratio and very good mechanical performance, properties that are determinant to their use in several applications such as air and liquid filtration, tissue engineering, optical and chemical sensors [12]. Although electrospunnanofibers have been used in industrial, consumer and defence filtration applications for more than twenty years, most of the research conducted to date has focused on synthetic polymers. Examples of electrospinning of natural polymers are limited to silk collagen, DNA, alginate, chitosan and more recently fibrinogen, gelatine and hyaluronic acid [13]. Electrospun composite nanofibers have attracted more attention recently in waste water treatment and dye removal due to their unique properties such as small fiber diameter, high surface area-to-volume ratio, high flexibility for chemical/physical surface modifications and physicochemical properties [14], which makes it ideal for many applications. Electrospun composite nanofiber can be used as either an adsorbent material [15], or for size-based separations such as microfiltration, ultrafiltration and even nanofiltration [16]. This research focuses on the preparation, characterization and performance evaluation of electrospun composite nanofibers were prepared by electrospinning using PVA, PEG blend solution crosslinked by GA. Electrospun blended nanofibers containing various ratios of GA concentrations were obtained.

The effect of GA on the morphology of fibers is studied. PVA/PEG/GA blends composite nanofibers were modulated by introducing molybdenum trioxide nanoparticles (MoO_3) nanoparticles and explored for sustainable contaminant removal. A PVA/PEG/GA-MoO_3 composite nanofiber was also investigated by the discoloration efficiency of methylene blue (MB) dye. The structure of the blended nanofibers containing GA and MoO3 was characterized and the swelling properties were measured. We examined the effects of numerous parameters, such as initial dye concentration, pH and contact time, on adsorption capacity. In addition, thermodynamic study and kinetic study in batch experiments of the PVA/PEG/GA-MoO_3 composite nanofibers are also investigated and discussed. The composite nanofibers showed appreciable removal efficiency of the target dye sorptives from a contaminated water.

MATERIALS AND METHODS

Materials: PVA, 98% hydrolysis (Mt. 72.000) were obtained from MerchSchuchardt OHG, Germany. Polyethylene glycol (PEG, Mt, 1200) and gluteraldehyde (GA, 25%) were purchased from Sigma–Aldrich (USA). Methylene Blue (MB) was used as model dyes (Figure 1). The commercially available dye MB was purchased from Merck, India. All other chemicals were of analytical grade and were purchased from Sigma.

Preparation of Crosslinked PVA/PEG/GA Blend: At first PVA powder was dissolved in distilled water by heating the solution at 85°C with vigorous stirring for 2 hr the concentration of PVA solutions tested was 8wt %, After the solution was cooled to room temperature and no particles remained, PEG (1wt. %) was added to the polymer solution at the desired ratio. The solution was mechanically stirred and heated at 70°C for 1 hr until completely homogenous. After that, the GA crosslinkedwith different concentration (0.5, 1, 1.5, 2, 3, 4 wt %) was gradually dropped into the above solution; the mixture was stirred for different reaction time (15, 30, 60, 90, 120 min) with vigorous stirring (Fig. 1A).

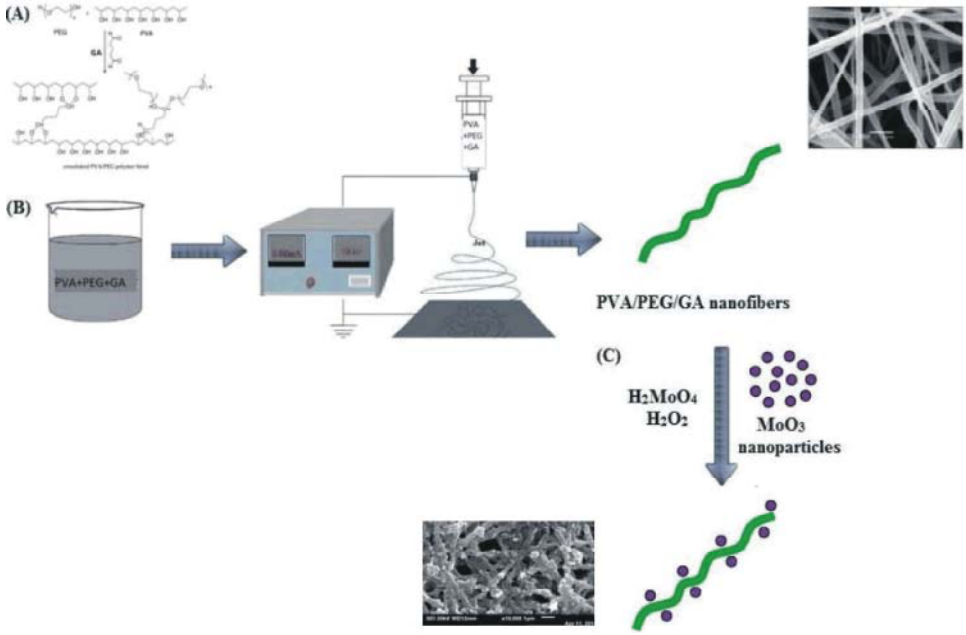

Fig. 1: Schematic diagram of A) PVA/PEG with GA, B) the electrospinning of nanofiber and c) PVA/PEG/GA with MoO3nanocomposite

Preparation of MoO3 Nanoparticles: The MoO3 nanoparticles prepared by using ion exchange a glass column with height of 100 ml and 30 ml in diameter was used for the cation-exchange process. The glass column was packed with 30 mL of the cation-exchange resin and then 10 mL of water was passed through the column to wash the resin .This washing step was repeated five times before the experiment The molybdic acid (H2MoO4) solution was prepared by successively by passing 50 mL aqueous solution of 0.1 mol/L of (Na2MoO4.2H2O) prepared by dissolve 6.17 g in 50 mL distilled water pass through columns of a ion-exchange resin this treatment allowed removing of Na+ ions from the solution. 30% H2O2 solution was added slowly to the H2MoO4 solution. The solution containing (0.1% H2O2) was evaporated at 60°C. The final powder obtained was annealing for 2 h at 300°C.

Electrospinning of PVA/PEG/GA Nanofiber: In this process the above mentioned PVA/PEG/GA solutions were placed into a 10 mL plastic syringe connected to a stainless steel needle. A high voltage is applied (20-25) KV The voltage is applied gradually and when the applied voltage overcomes the surface tension of the polymer solution (Fig. 1B), a Taylor cone appears and it spins down as a fiber to reach the collector. The collector was covered with aluminum foil and the nanofibers were collected on it at room temperature. Before reaching the collector, the solvent evaporates and the polymer solidifies and gets collected as fibers. The distance between the needle tip and collector was fixed at 10 cm. The feed rate was chosen to be 0.1 mL/hr. Then nanofibers were dried for 24 hr at room temperature. After the polymer PVA/PEG/GA nanofibers prepared we deposited it in the solution of (H_2MoO_4, H_2O_2) during the deposition of MoO3 nanoparticles and allow it to deposit on the nanofiber.

Nanofibers Characterization: The surface morphologies of the electrospun PVA/PEG/GA nanofibers were assessed via a scanning electron microscope (SEM, JEOL GSM-6610LV. Japan) operating at acceleration voltage of 20 kV. Specimen surfaces were coated with a thin layer of gold before observed. The fiber diameter of the electrospun fibers was measured using Image J software from the SEM pictures in original magnification. At least 100isolated nanofibers were randomly selected and their diameters and diameter distributions were measured and averaged. FT-IR of blend nanofibers was recorded by a Fourier transform infrared spectrometer (FTIR, Shimadzu FTIR-8400 S, Japan) FTIR spectra. The experiments were carried out in the range of 4000 to 400 cm^{-1}. The infrared spectra were recorded in the transmission mode using thick mats of electrospunnanofibers. Thermal stability of electrospinningnanofibers was characterized using Thermo-Gravimetric Analyzer (Shimadzu Thermal Gravimetric Analysis (TGA)-50, Japan). All measurements were performed under a nitrogen atmosphere with a flow

rate of 10 mL/min by heating the material from 25°C to 600°C at a heating rate of 10°C min^{-1}. The water content of the nanofibers after swelling value (S) was calculated using equation (1) [12]:

$$S = wa\text{-}wdwdX100 \quad (1)$$

where (Wa) was the water up-take per gram of the nanofibers and (Wd) and (Wa) were the weight of the nanofibers after swelling and subsequent drying, respectively. The time duration for Swelling was (15, 30, 60, 120, 240, 360 and 1440 min). The excess water on the swollen fibers was wiped out with a filter paper. Each sample for swelling should be checked in 3 times. The mechanical properties of PVA/PEG/GA blend nanofibers were characterized using a tensile tester (model AG-I, Shidmadzu, Japan) according to ASTM ID: D882-12. Specimens with 6 mm× 1 mm dimensions were cut and used for analysis at a crosshead speed of 30 mm/min. The specimen thicknesses were measured using a digital micrometer (Mituto, Tokyo, Japan), having a precision of 0.001 mm. Sheets strips were fixed between the grips and the crosshead speed was set at 30 mm/min. The average values from five repetitions were taken as the tensile strength and strain at break results.

Adsorption Experiments: To evaluate the adsorption performance of PVA/PEG/GA-MoO3 composite nanofiber for MB dye adsorption in aqueous solution, the influence of the several parameters, that is, nanocomposite dosage, initial dye concentration, initial solution pH and contact temperature were conducted in a batch mode of operation at the equilibrium time of 60 min at room temperature. Generally, all adsorption experiments were performed in batch mode at 150 rpm in shaker bath operating at 25°C. Dye removal ability of 3X3 cm2 (0.09 g) from the fabricated composite nanofibers were added to 50 mL glass bottles containing initial dye concentration (20 mg/L) MB. The glass bottles were wrapped with aluminum foil to avoid light exposure and mixed using thermostatic shaker bath at 150 rpm for 60 min at 25°C. MB concentrations before and after adsorption analyzed using a UV–Vis spectrophotometer (T80 + UV/Vis spectrometer, PG Instruments Ltd, UK) at wavelength of 668 nm via standard calibration curve. The dye removal efficiency onto the PVA/PEG/GA-MoO3composite nanofiber can be calculated using the following equation:

$$\% \text{ Removal} = C\text{-}C\ C\ X100 \quad (2)$$

where C and C are the initial and equilibrium liquid phase concentrations of MB, respectively ($mg.L^{-1}$). All of the experiments were performed three times.

Kinetic Sorption of Dye onto Composite Nanofiber: MB dye was selected to evaluate the pure PVA/PEG/GA-MoO3composite nanofiber adsorption capacity. The influence of contact time on the MB dye adsorption was monitored using 3X3 Cm^2(0.09 g) of composite nanofiber were added to 50 mL MB of specified initial dye concentration solution (1–50 ppm) that was mixed with at 400 rpm for different time intervals. 2 mL aliquots were drawn at predetermined time intervals and analyzed using the spectrophotometer.

Equilibrium Sorption of Dye onto Composite Nanofiber: The effect of dye solution concentration was monitored in a batch experiment of operation at the adsorption equilibrium time of 30 min. The equilibrium adsorption capacities of PVA/PEG/GA-MoO3composite nanofiber data were modeled using the linear forms of Langmuir and Frendlich equilibrium isotherm models.

RESULT AND DISCUSSION

Characterization of Nanofibers

Effect of GA on the Morphology of the Resultant Nanofibers: The effects of the different concentration of GA on the solution properties of PVA/PEG/GA blends and on the morphology of the resultant nanofibers were studied using a scanning electron microscope (SEM). The surface morphology of electrospunnanofibers are presented in Fig. 2A-F. According to the SEM images, the surface morphology and the average diameter of the nanofibers are dependent on initially added GA concentrations. GA is a more effective crosslinking agent than other aldehydes [17]. When the concentration of GA increased the nanofibers morphology changed and the fiber become continuous and enhanced fiber-structures. as show in Fig. 2 as the concentration of GA increase from 0.5 to2 wt% the fiber diameter decrease from (360.06 ±111.70 to 166.76 ±51.59) then fiber diameter increase as the concentration of GA reached to 4% (237.41± 61.85) that is due to the cross-linked of fibers show a wider distribution, indicated by the increased standard deviation, due to the constantly changing viscosity of the electrospinning sample [18].

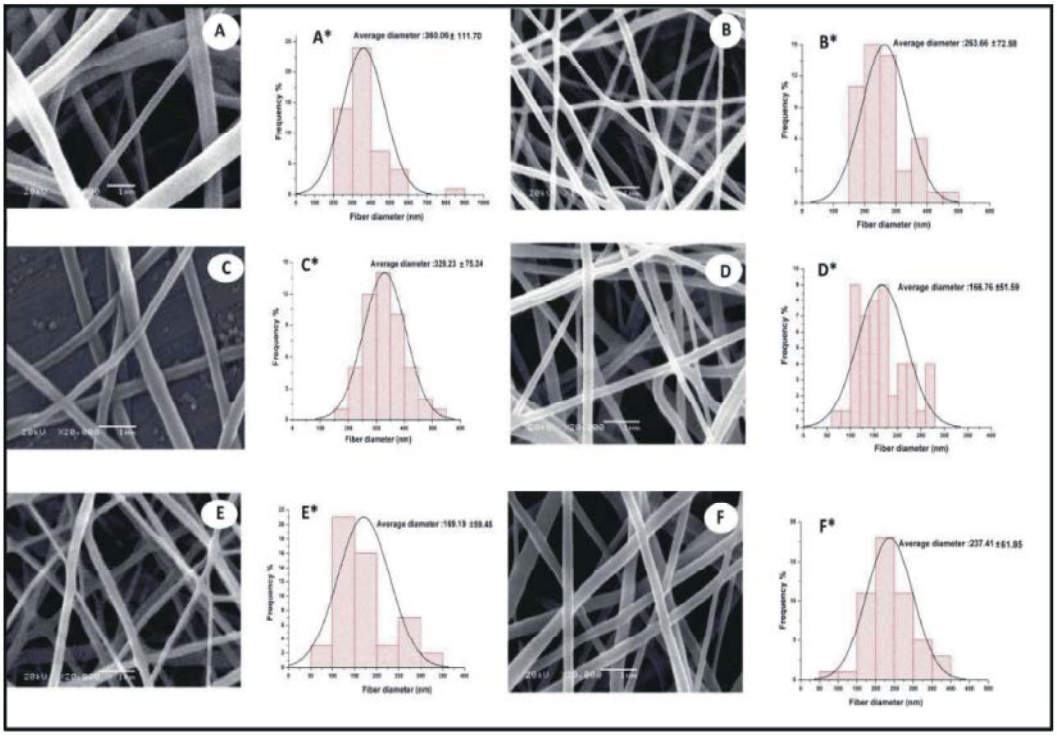

Fig. 2: SEM photographs and distribution of the average diameter of PVA/PEG/GA nanofibers with various concentration of GA, (A)0.5%, (B) 1%, (C) 1.5%, (D) 2%, (E)3% and (F) 4%

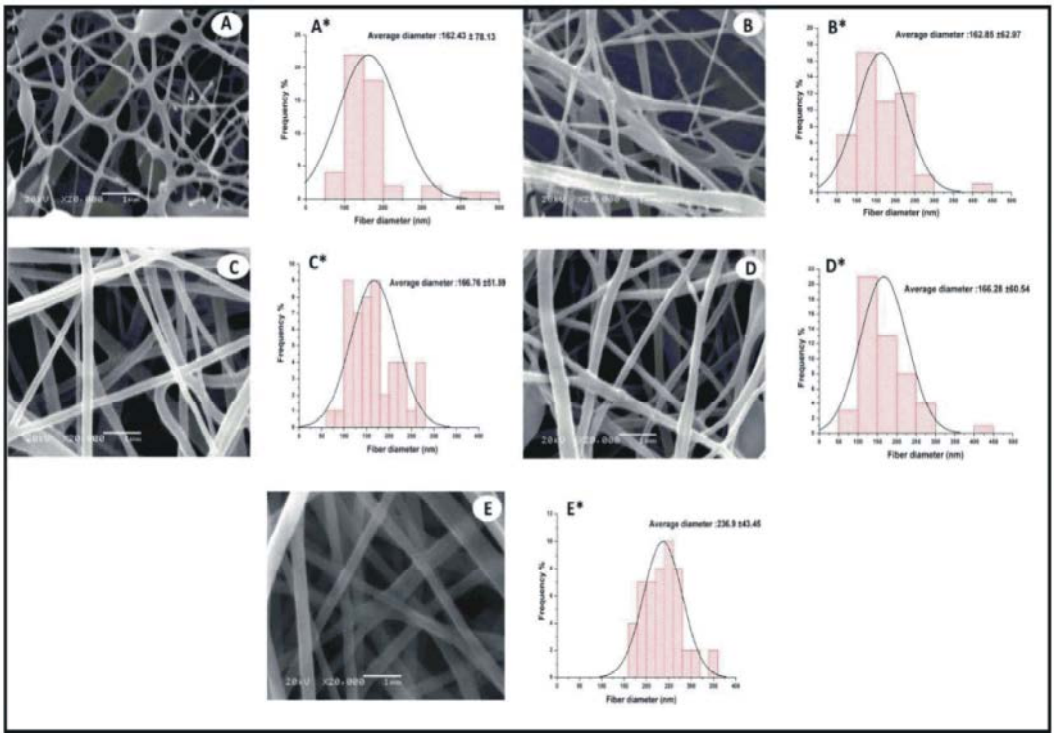

Fig. 3: SEM photographs and distribution of the average diameter of PVA/PEG/GA nanofibers with various reaction times with GA, (A) 15, (B) 30, (C) 60, (D) 90 and (E)120 min.

Fig. 3 shows SEM morphology and diameter distribution of PVA/PEG/GA blend nanofibers with various reaction times with GA. The increase in the time of crosslinking effect on the morphology and average diameter and distribution of the nanofibers. When the reaction times with GA increased the nanofibers morphology changed and the fiber become continuous and enhanced fiber-structures. Also, the amount of nanofibers cross linked increased and the nanofibers morphology changed [19] and the fiber diameter increase from (162.43 ±78.13 to 236.9 ±43.45). Moreover, the distribution of the PVA/PEG/GA blend nanofiber became broader. This behavior mainly attributed to the charge density increases in the PVA/PEG/GA blend solutions during electrospinning, resulting in strong electrostatic repulsion among the sprays. This repulsive force easily overcomes the surface tension of the jet to reduce diameters of the nanofibers [20].

Swelling Properties: The swelling property of PVA/PEG/GA nanofiber was studied in water with different GA concentrations (0.5–4%) for different time periods (15 and 1440 min). Differences in swelling tendency are shown in Figure 4. It was observed that the effect of cross-linking is still more important, swelling ratio for PVA/PEG with 1, 1.5 and 3% GA more than 500% after 1 hour. After that the nanofibers showed a slight decrease in the swelling ratio as the length of exposure was increased. The presence of a large number of hydroxyl groups in nanofiber results in strong hydrogen bonding (may be of both intermolecular and intermolecular types), which in turn affects the solubility of nano fiber in water [21]. When PVA/PEG nanofibercrosslinked with GA formation of acetyl bridges between the aldehydes ends of the GA and the hydroxyl groups of nanofibers both in intermolecular and/or intermolecular fashion occurred within and at the point of contact between nanofibers.

We also observed that with the increase in GA concentration and the crosslinking reaction time the nanofiberscrosslinked increased. Also, when the GA concentration increased from 0.5% to4wt % the SEM micrograph showed swollen fiber network and the morphology of nanofibers changed with increased cross-linking time, thenanofibers became more swell [21]. Figure 4B indicates the swelling results of PVA/PEG/GA nanofiber in water with different GA reaction times (15 and 240 min). As shown in Fig. 4B a higher swelling and water uptake ability were observed for the PVA/PEG/GA nanofiber after 15 min reaction time with GA. PVA/PEG/GA nanofiber exhibited a completely swollen morphology that may be due to the hydrophilic properties of PVA/PEG/GA crosslinkednanofiber. However, the PVA/PEG/GA crosslinkednanofiber with reaction time 240 min showed a lower swelling ratio compared to reaction time 15 min. increasing the crosslinking time from 15 min to 1440 min decreased their swelling capabilities noticeably from 1200 to 400 %. The reduced fiber swelling in the PVA/PEG/GA crosslinkednanofiber may be a result of increased PVA/PEG/GA nanofiber hydrophobicity reducing the interaction of the aqueous medium with the fibers.

Mechanical Properties: The tensile strength of the PEG with PVA in various blend ratios nanofibers was analyzed using a universal material testing machine. Figure 5A show the stress-strain of of PVA/PEG/GA nanofiber with different concentration of PEG increased from 0.1 % to 1.5%, from which could be noticed that the stress properties seemed to become superior after the addition of PEG increased.PEG blended with PVA has been reported to have good mechanical and chemical properties and, The enhanced property has been attributed to the interactions between PEG and PVA in the blend through hydrophobic side-chain aggregation and intermolecular and intra-molecular hydrogen bonds as shown in Fig. 5A. The mechanical behavior of electrospun blend nanofiber depended on the nanofiber structure; properties of the polymer blend constituents and the interaction between each polymer nanofiber [22]. It could be seen that the tensile strength was increased obviously from (4.4 to 7.5) MPa. Whenthe mass ratio of PVA/PEG was increased, the stress value increase and the elongation value decrease. So, the blended fiber exhibited much higher tensile strength values [23].

Also, Fig. 5B showed typical tensile stress–strain data PVA/PEG/GA nanofiber for with different GA concentrations (0.5–4%). It is known that crosslinking of polymers would improve their mechanical properties [24, 25]. The tensile strength indicates that GA crosslinking made nanofiber became mechanically more strong and stable. In addition, the interfere bonding of nanofiber occurring mostly at intersection points were also reported to improve the mechanical and physical properties of the crosslinked polymer by providing a rigid web of inter fiber bonding [26]. Fig. 5B show that the tensile strength of the PVA/PEG/0.5% GA nanofiber was measured to be 5.27 MPa and its ultimate strain was 83.12%, whereas after the concentration of GA

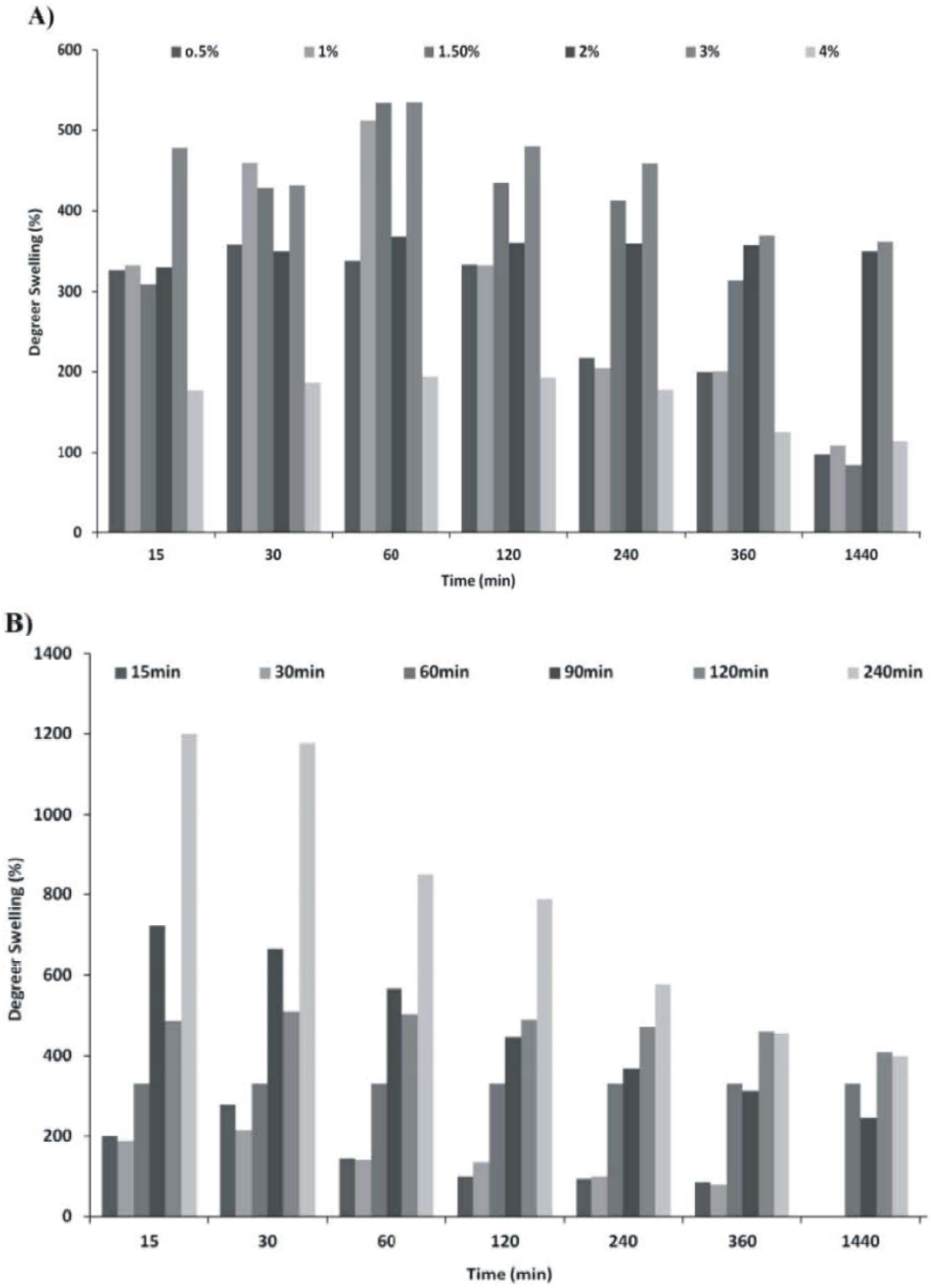

Fig. 4: Swelling properties of PVA/PEG/GA nanofiber: A) with various GA crosslinking, B) with various GA crosslinking reaction times

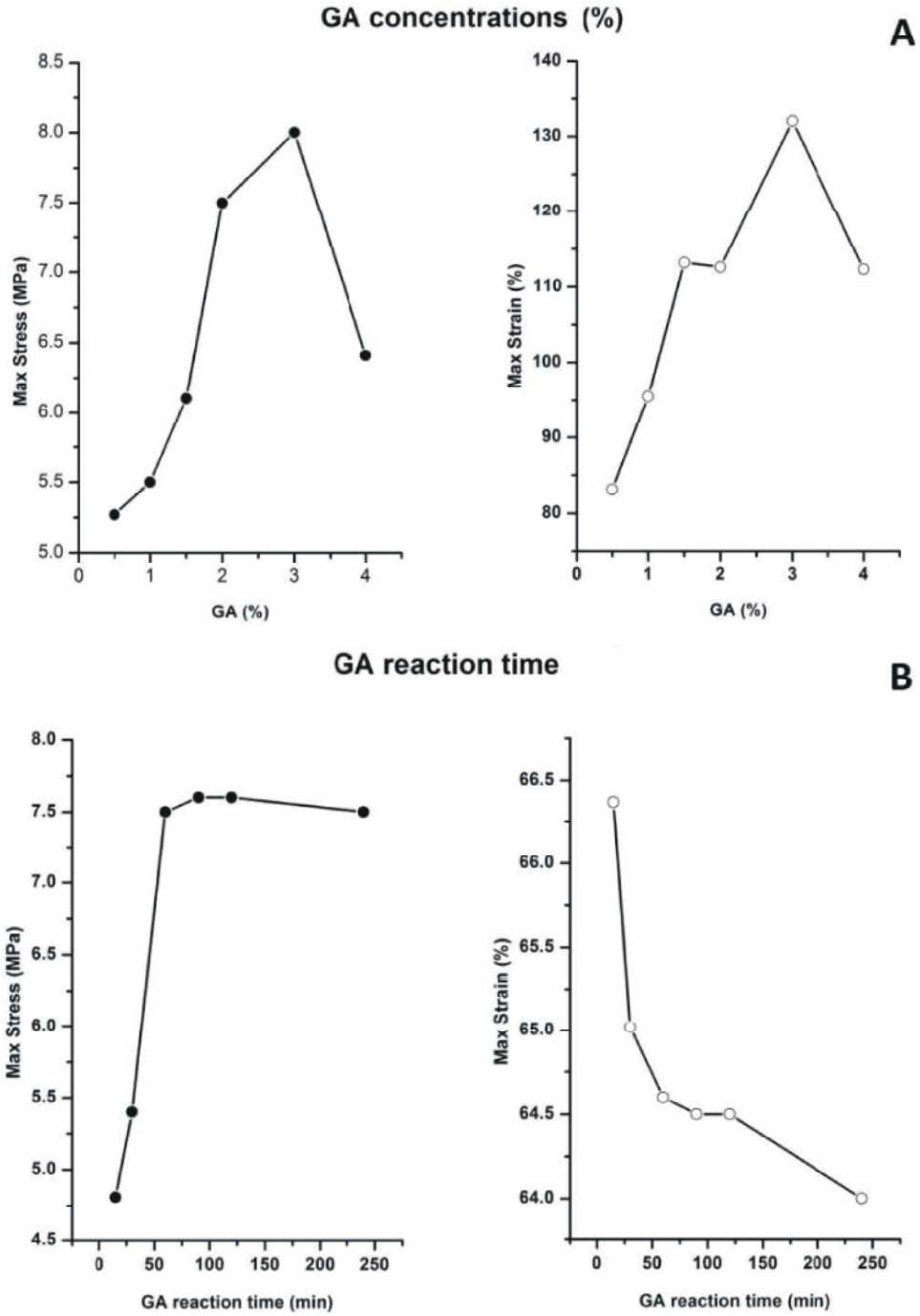

Fig. 5: Mechanical properties of of PVA/PEG/GA nanofiber: A) with various GA crosslinking, B) with various GA crosslinking reaction times.

cross-linker increase to 3%, the tensile strength of the PVA/PEG/3% GA nanofiber increased for about 8 MPa and the elongation value decrease. The enhanced tensile strength indicated that crosslinked PVA/PEG nanofiber became mechanically more strong and stable. On the other hand, the mechanical properties of the PVA/PEG/GA nanofiber in water with different GA reaction times (15 and 240 min) are evaluated by the tensile strength measurements.

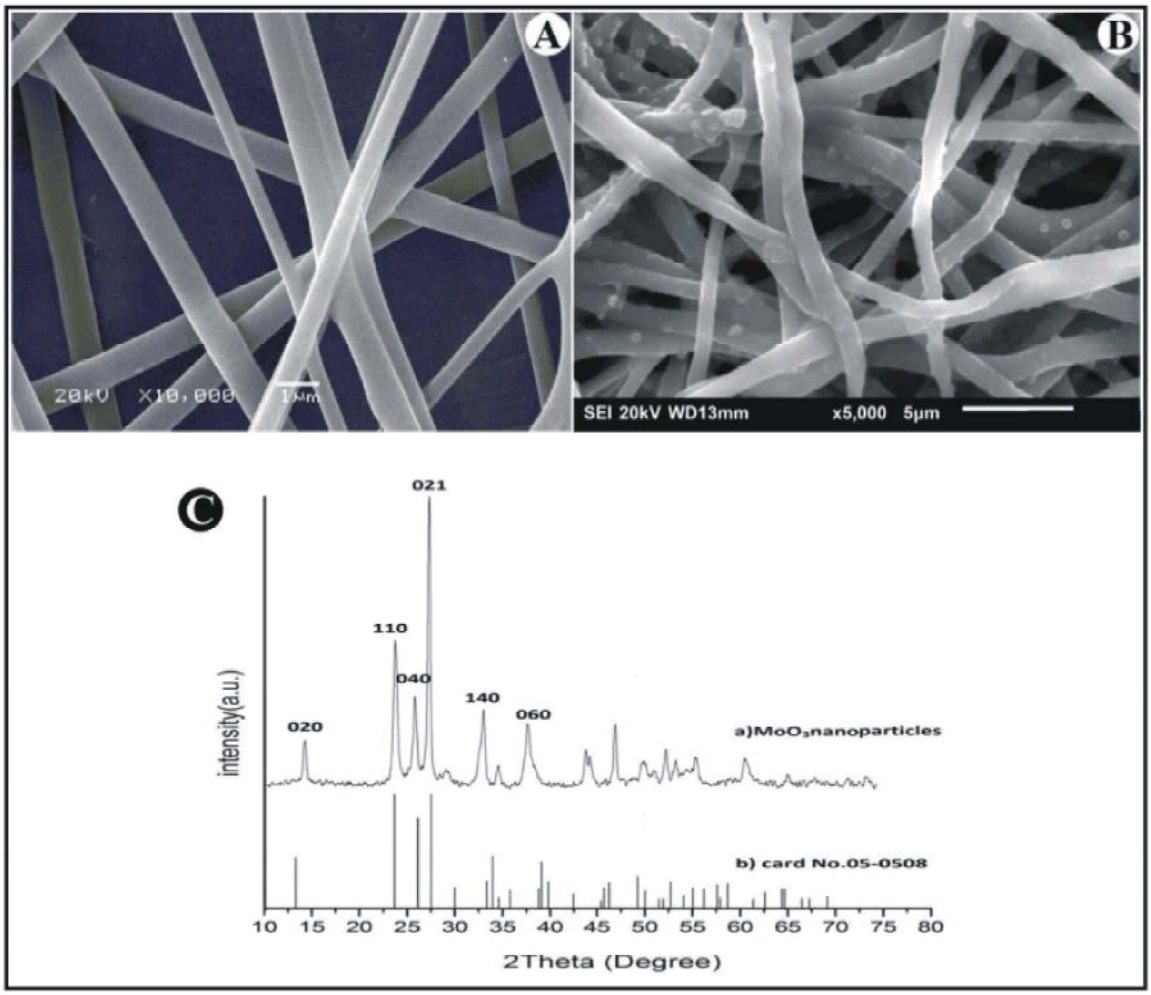

Fig. 6: A) SEM photographs of PVA/PEG/GA nanofibers, B) PVA/PEG/GA- MoO3nanofibers and C) XRD patterns of the MoO3 NPs and The orthorhombic and JCPDS card No.05-0508.

X-Ray Diffraction Analysis and Morphology of Crosslinkednanofiber Containing MoO_3 NPs: The surfaces morphology of the crosslinkednanofiber without MoO_3 NPs and crosslinkednanofiber with MoO_3 NPs was observed by SEM (Fig. 6A and B). It was found that the surface of the electrospun pure fiber is very smooth, non-beaded surfaces (Figure 6(A)). Fig. 6 B represents the crosslinkednanofiber with MoO_3 composite nanofiber, the composite fibers arranged at random and some spindle-like beads appeared on the fibers. At the same time, the average diameter of the composite nanofibers was the largest among the pure fiber mats; the average fiber diameter has risen by about 10-20% of the pure fiber diameter. On the other hand, the crystal structure of the sample is further determined by X-ray diffraction (XRD) with the JCPDS files, as shown in Fig. 6C. All the identified peaks can be assigned to α-MoO3 (orthorhombic system, JCPDS card No.05-0508) [27]. The stronger intensities of the (020), (040) and (060) diffraction peaks of the sample than those of other peaks, suggesting a layer crystal structure or a highly anisotropic growth of the nanostructures [28, 29] Peaks due to other phases are not identified in the sample, indicating high purity of the as-synthesized α-MoO3 NPs[30].

FTIR Spectrum of Composite Nanofiber and TGA of Composite Nanofiber: FTIR spectrum of pure PVA reference shown in Fig. 12a the major peaks associated with PVA for instance, it can be observed (C–H) broad alkyl stretching band (2850–3000 cm^{-1}) and typical strong hydroxyl bands for free alcohol no bonded (–OH) stretching band at (3600–3650 cm^{-1}) and hydrogen

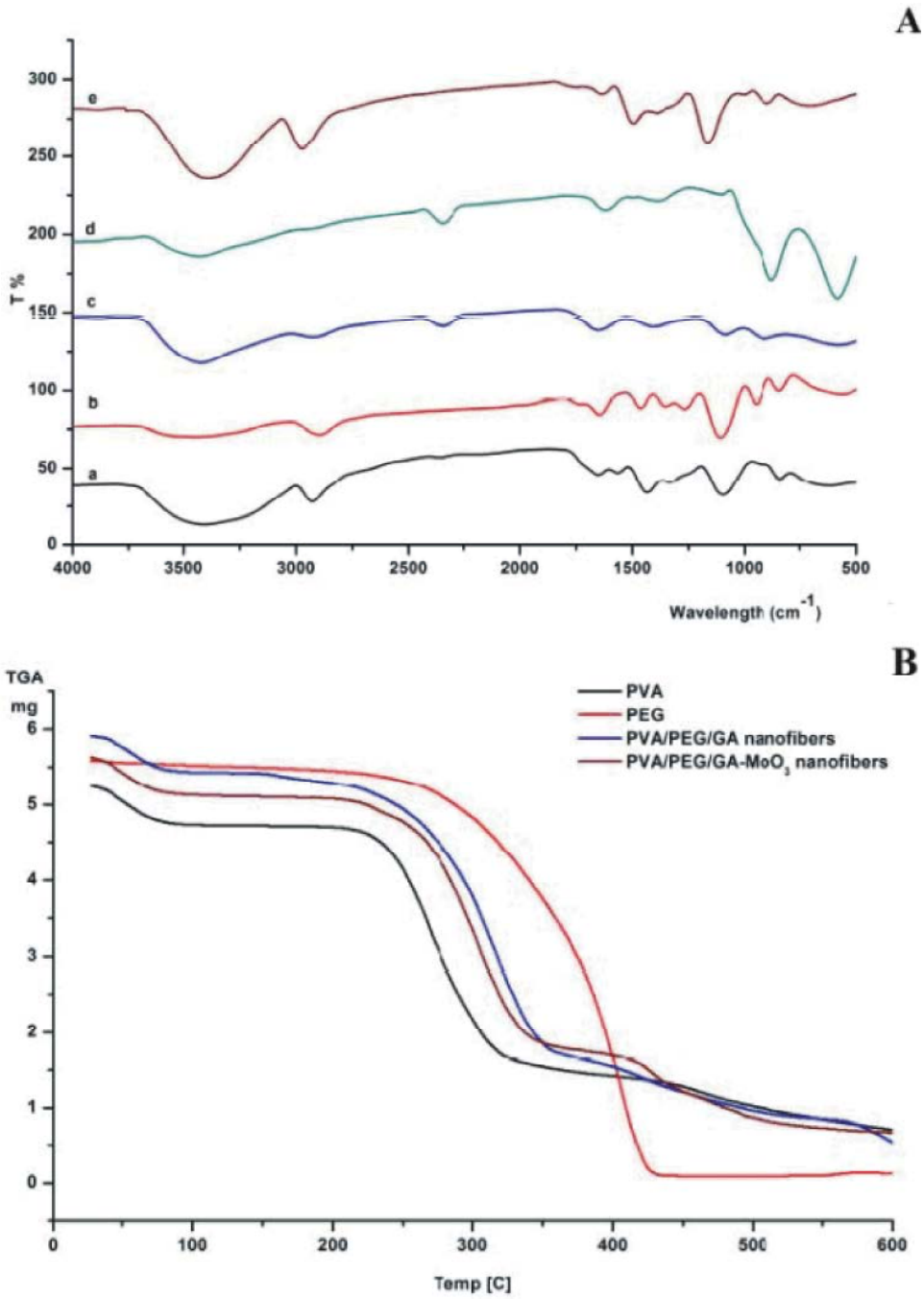

Fig. 7: A) FTIR spectra of (a) PVA, (b) PEG and (c) MoO3 nanoparticles, (d) PVA/PEG/GA nanofibers and (e) PVA/PEG/GA-MoO3 composite nanofibers and B) TGA thermograms of (a) PVA, (b) PEG and (c) PVA/PEG/GA nanofibers and (d) PVA/PEG/GA-MoO_3 composite nanofibers.

bonded band (3200–3570 cm^{-1}) [31] Intra molecular and intermolecular hydrogen bonding are expected to occur among PVA chains due to high hydrophilic forces. An import absorption peak was verified absorption band(C-O) at 1142 cm^{-1} has been used as an assessment tool of poly (vinyl alcohol) structure because it is a semi crystalline synthetic polymer able to form some domains depending on several process parameters [32].

In Fig. 7A, the IR spectra of PEG have exhibited important absorption bands from FTIR spectroscopy measurements as shown in the figure. It was verified contributions associated with stretching of ether groups [33]; from (1050 to 1150 cm^{-1}) with maximum peak at 1150 cm^{-1}. Characteristic alkyl (R–CH2) stretching modes from (2850–3000 cm^{-1}) were observed [34].Also, (OH) hydroxyl group contribution was observed with absorption ranging from (3200–3600 cm^{-1}). It should be noted that the presence of hydrophilic and hydrophobic moieties in poly ethylene glycol chains verified by FTIR spectroscopy generally gives them a unique ability of to be solublein both aqueous and organic solvents. As a consequence, PEG is widely used separated, conjugated or blended with other polymers such as PVA [32]. Fig. 7Ac shows FTIR spectroscopy for the blend fiber with GA. The large broad band observed at (3200-3650 cm^{-1}) are associated with the stretching vibration of hydroxyl (-OH) group from intermolecular and intra molecular hydrogen bonds and their intensity were observed relatively decreasing when compared to electro spun PVA nanofibers mat as the cross-linking increases indicating that more of the -OH groups are involved in the formation of acetyl bridge. The two vibrational bands observed between (2730 and 2860 cm^{-1}) refer to the stretching vibration of C-H from alkyl and O=C-H from the aldehyde and the bands between (1700 and 1750 cm^{-1}) are due to the C=O stretching of the unreacted end of the aldehyde in the cross-linked PVA, PEG nanofiber. The band observed at (1000-1140 cm^{-1}) with gradual broadening of the peak width as the cross-linking reaction time increase is attributed to O-C-O vibration of the acetyl group [35]. Figure 7B shows the TGA of PVA, PEG and PVA/PEG/GA nanofibers. TGA is a powerful technique, usually employed for the analysis of the decomposition and thermal stability of materials. TGA measures the weight change as a function of temperature. As the temperature increases, the weight of the sample decreases, indicating the continuous composition of the sample In the TGA thermogram. The PVA nanofiber lost about 8% mass at temperatures up to 77°C due to the evaporation of absorbed moisture Fig 7Ba, the decomposition of PVA began around 218°C and lost half of its mass at 324°C, leaving merely 5%residueat 600°C. The TGA thermogram of PEG nanofiber Fig 7Bb showed slightly lowered moisture absorption as well as onset temperature of decomposition It lose about 3% at 229°C leaving 6% residue at 431°C. The extents of lowered moisture absorption and onset decomposition temperature of decomposition were generally increased with longer PEG chain lengths and higher PEG contents. Also, Fig. 7Bc illustrates the TGA of the crosslinked PVA/PEG/GA nanofiber, the first region at a temperature of 80°C the sample loss of 7% it was due to the evaporation of free and bound water. The transition region at around 206-356°C loss about 59% was due to the degradation of the GA, leaving merely 5% residueat 600°C. The slight shifting represents the increase in the thermal stability which probably ascribed to the formation of crystalline polymer matrix as a result of cross-linking between the two polymers and formation of interpenetrating polymer network structure.

Adsorption Activity of PVA/PEG/GA- MoO3 Composite Nanofibers: The effects of various parameters affected the removal of MB dye by PVA/PEG/GA-MoO_3 composite nanofibers such as contact time, adsorbent dose concentration, temperature and pH has been evaluated and optimized in the batch method experiments.

Effect of Dye Concentration: The influence of the MB dye concentration on the rate of adsorption behavior of PVA/PEG/GA-MoO3 composite nanofibers was studied and the results are shown in Fig. 8a. The experiments were carried out at fixed adsorbent dose (20 mg) of powder with 5 ml aqueous solution of MB dye at different concentrations (50, 75, 100, 150 and 200 mg L^{-1}) as initial amounts for 60 minutes at room temperature and (pH7). Generally, it is clear from the figure that the percent adsorption increase with the increase in initial dye concentration, until reached to100 mg L^{-1} then decrease as shown in Fig. 8a. It means that the adsorption is highly dependent on the initial concentration of dye [36], which may be due to the ratio of the high initial concentrations of MB dye molecule to the available adsorptive surface sites is low, subsequently; the fractional adsorption becomes independent of the initial concentration. However, at high concentration the available sites of adsorption becomes fewer and hence, the percentage removal of dye is dependent upon the initial concentration [37]. It was revealed that, the maximum uptake of MB was observed when 100 mg L^{-1} of dyes concentration was employed, as shown in Fig. 8a. Therefore, for the rest of the experiments 100 mg L^{-1} dyes concentration was selected as the main concentration for investigating the following parameters.

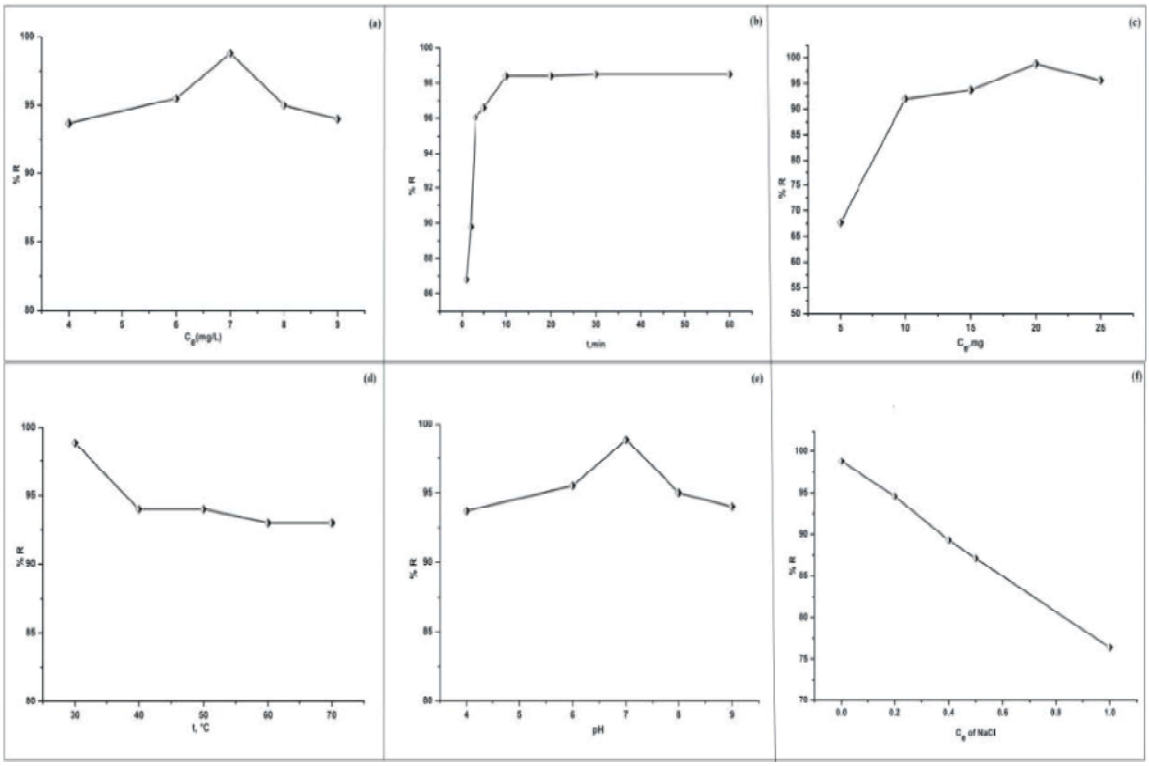

Fig. 8: Factors affecting the removal process: (A) initial MB concentration, (B) contact time, (C) adsorbent doses, (D) Temperature, (E) pH and (F) NaCl concentration.

Effect of Incubation Time: In the adsorption system contact time plays a vital role irrespective of the other experimental parameters affecting the adsorption kinetics. In order to study adsorption of MB by PVA/PEG/GA-MoO3 composite nanofibers the adsorption experiments were carried out at different contact time (1-60min) as show in Fig. 8b at constant initial concentration of dye (100 mg L^{-1}) with a fixed dose of adsorbent (20 mg). It is found that the removal of MB increases with increase in contact time. As show on the Fig. 8b, the rate of MB dye removal was very fast, where 98% of the dye was removed within 10 min. So, 10 min was selected as the best contact time for MB dye removal.

Effect of Adsorbent Doses: Influence of variation the initial adsorbent doses of PVA/PEG/GA-MoO3 composite nanofibers was studied in the range 5–25 mg as shown in Fig. 8C, the percentage of dye removal was enhanced by increasing an adsorbent dose, as shown in Fig. 8c. Increase in the adsorption with adsorbent dosage can be attributed to increased surface area and availability of more adsorption sites [37], the maximum uptake of MB was observed when an adsorbent dose was 20 mg. Thus, 20mg was selected as the best dose for MB dye removal, as shown in Table (3.9).

Effect of Incubation Temperature: The effect of solution temperature is one of the major factors, which effect on MB removal (%) process. The effect of solution temperature on the adsorption of MB dye by PVA/PEG/GA-MoO_3 composite nanofibers was studied and investigated by performing the adsorption experiments at different temperatures in the range between (30-70°C) and the results were presented Fig. 8d. The experimental results showed that the maximum uptake of MB was observed at temperature 30°C as shown in Fig. 8C. When the temperature was higher than 40°C, the MB removal (%) decrease with the increasing of temperature and increasing the temperature from 40 to 70°C accompanied by a gradual decrease of the percentage of MB dye compound adsorbed and removed from the solution by PVA/PEG/GA-MoO_3 composite nanofibers. Higher temperature will lead to lower diffusion rate of the dye into the composite nanofibers and decrease the decolorization efficacy. Also, increase in temperature due to decreased surface activity [38].

Effect of pH: Fig. 8e shows the effect of pH on dye removal. The solution pH is one of the principal parameters which controlling the adsorption process. The effect of solution pH on the MB dye adsorption by PVA/PEG/GA-MoO_3 composite nanofibers was therefore explored in the pH range from 4.0 to 9.0. At pH pH from 4.0 to 7.0 accompanied by an increase in the adsorption percentage from 93.7% to 98.8%. Therefore, the adsorption capacity of the polymer gradually decreases and reaches a minimum with the increase of pH range from 8.0 to 9.0. These phenomena could be due to the surface charge and attraction forces of between the negatively charged PVA/PEG/GA-MoO_3 composite nanofibers surface and the positively charged MB dye.

Effect of Salt Concentration: As shown in Fig. 8f, the MB dye adsorption process on PVA/PEG/GA-MoO_3 composite nanofibers and the effects of NaCl content in the adsorption solution on its MB dye adsorption capacity and removal efficiency (%). It is clear that the adsorption capacity decreased with the increase of NaCl concentration. It can be explained that the adsorption occurred mainly due to the conductivity of dye solutions and addition of the salt to change solution conductivity leads to addition of impurity in wastewater and leading to the declined adsorption capacity.

Equilibrium Isotherm Analysis of MB dye Adsorption Process: The isotherm study was carried out with the same operating conditions as the equilibrium studies. The effect of dye solution concentration was monitored through batch experiments of operation at the adsorption equilibrium time of 30 min. The equilibrium adsorption capacities of PVA/PEG/GA-MoO3composite nanofiber were described by Langmuir and Frendlich isotherm models. They are listed below:

Langmuir Model:

??????????=1Q?b+?????Q? (2)

where Ce is the equilibrium concentration of dye in solution (mg/L), qe is the amount of dye adsorbed at equilibrium time (mg/g), b is the Langmuir constant related to binding energy of the adsorption system (l/g.) and Q? is the Langmuir constant. The values of Q? and b were obtained from the slope and intercept of the plot, Ce/ q? versus Ce respectively. RL - The essential characteristics of the Langmuir isotherm can be expressed in terms of dimensionless equilibrium parameter RL, given by following equation (3)

????????=1/(1+???? ?????) (3)

where *K*L is the Langmuir constant (L/mg) and C? is the initial concentration of MB (mg/l). The *R*L value indicates whether the adsorption process is irreversible (*R*L = 0), favorable (0 < RL< 1), linear (*R*L = 1) or unfavorable (*R*L> 1).

In this model, when Ce/qe was plotted against Ce, straight line with 1/ Qo was obtained as shown in Figure 9A. The resulted slope indicated that, the adsorption of MB molecules on PVA/PEG/GA-MoO_3 composite nanofibers follows Langmuir isotherm model. As showed in the Figure 9A, the data of Langmuir isotherm model proved the homogeneity nature of the surface of nanofiber composite. This homogeneity is like to be each dye molecule / nanofiber composite adsorption has equal adsorption activation energy. The resulted data also illustrated formation of monolayer of dye molecules over the surface of nanofiber composite [39]. The essential characteristics of the Langmuir isotherm can be expressed in terms of dimensionless equilibrium parameter RL, (eq.4). The RL values for the adsorption of MB on nanofiber composite is observed in the range of 0-1, indicating that the adsorption was a favorable process.

Freundlich Model:

???????? ?????=???????? ????????+1???????????? ????? (4)

where Q? is the dye adsorbed (mg/g) at equilibrium, C? is the equilibrium concentration (mg/L), Kf (mg/g) is Freundlich constant indicating adsorption capacity and n is Freundlich constant indicating adsorption intensity. The values of Kf and n can be calculated from the intercept and slope of the plot ln q? versus log C?.

Fig. 9B shows Freundlich adsorption isotherm of MB dye onto PVA/PEG/GA-MoO_3 composite nanofibers adsorption. For this model, when log qe versus against log Ce gave a straight line with a slope 1/n, as shown in the previous figure 9B. This slope proved that the adsorption of MB dye using nanofiber composite also follows the Freundlich isotherm. As illustrated in the previous table, the data of Freundlich isotherm model indicates that Freundlich isotherm model was unsuitable for experimental data than other isotherms where n and

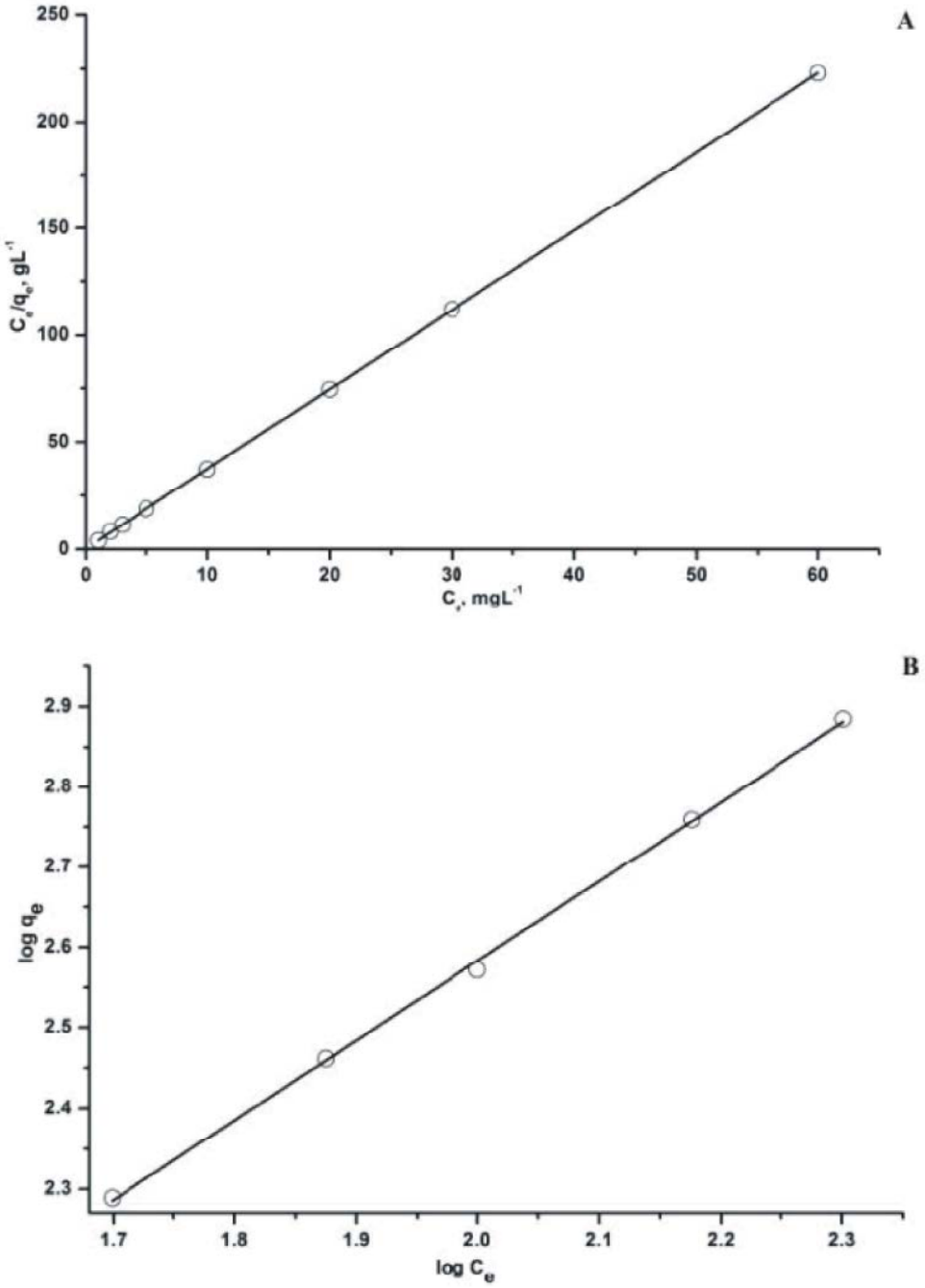

Fig. 9: A) Langmuir adsorption isotherm model and B) Freundlich adsorption isotherm model for dye adsorption process onto composite nanofibers.

Kf ((mg/g) (L/mg) 1/n) are Freundlich constants related to the favorability of adsorption process and the adsorption capacity of the adsorbate, respectively. If 1/n<1, it indicates a favorable adsorption. It can be seen that Figure 9B the values of 1/n are smaller than 1. Thefavorability of the adsorption process was further confirmed by the result [39]. The value of n is greater than unity (n = 3.7) indicating that the dye is favorably adsorbed by nanofiber composite. The parameters of the isotherm models were calculated from the experimental data and the values of correlation coefficient (R2) are presented in Table (3.15) (3.16). According to the results,

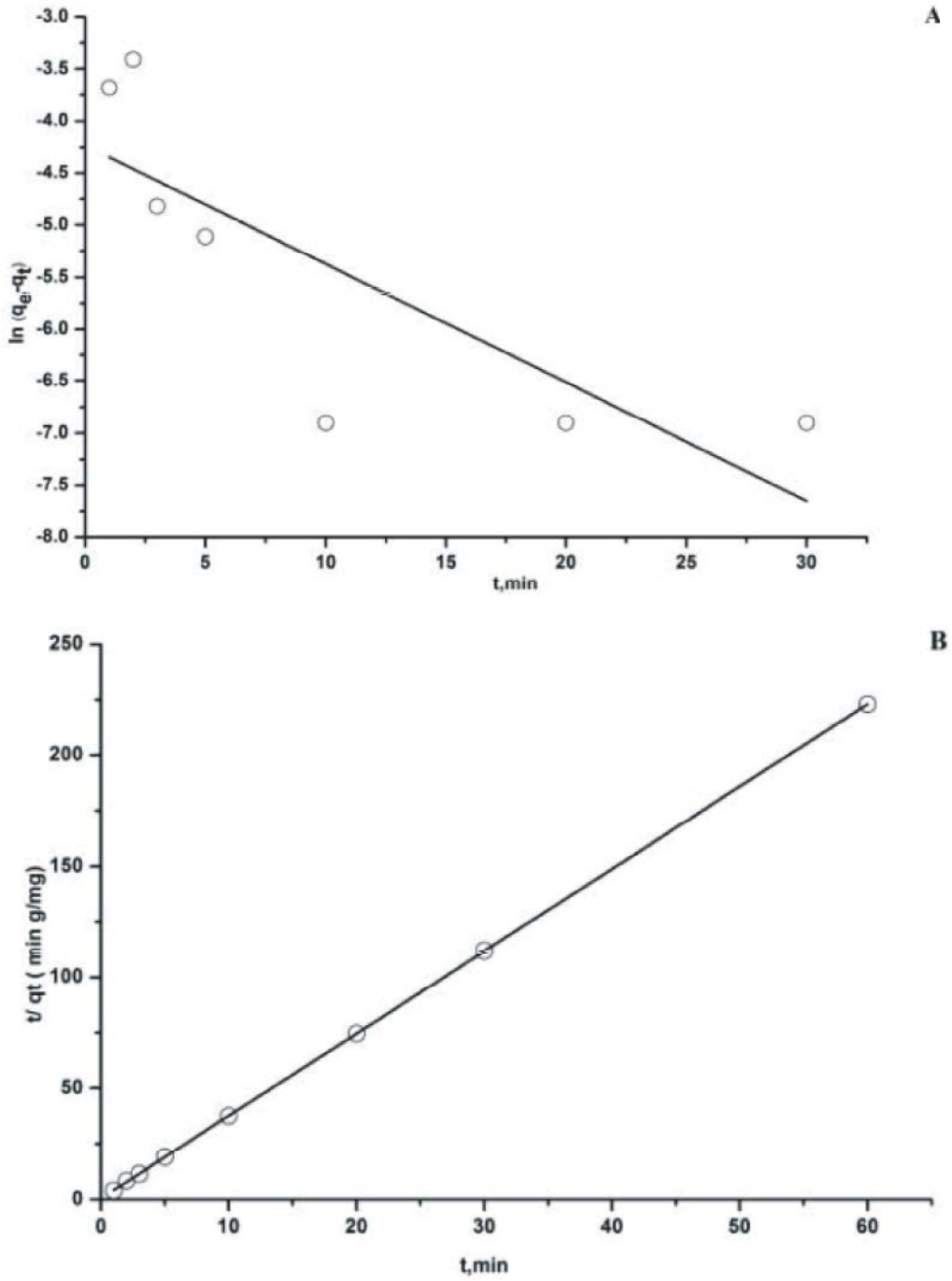

Fig. 10: A) Pseudo-first-order kinetics and B) Pseudo-Second Order for dye adsorption process onto composite nanofibers

Table 1: Comparison of kinetic parameters of dye adsorption onto composite nanofibers

Dye concentration (mg L^{-1})		*q*e, exp (mg g1)		First-order kinetic model		Second-order kinetic model	
*K*1 (Sec^{-1})	*q*e, cal (mgg^{-1})	*R2*		*K2*(g (mg Sec^{-1}))	*q*e, cal(mgg^{-1})	*R2*	
50	0.269	0.0087	68.91	0.99	27.16	0.296	1

the R2 values for the Langmuir higher than those in Freundlich isotherm model. It is clear that the equilibrium adsorption data comply with Langmuir isotherm model, which suggests that the adsorption is a process which occurs in a homogeneous surface. Additionally, these results also demonstrated no interaction and transmigration of dyes in the plane of the neighboring surface [39]. So, the Langmuir model yielded a better fit (R2 = 1) than the Freundlich model (R2 = 0.35).

Kinetic Model of MB Dyes Adsorption Process with Composite Nanofiber: The experimental results were tested using two kinetic models (Pseudo first-order and Pseudo second-order) were chosen to explain the adsorption mechanism of MB on composite nanofiber. These equations were listed below: *Pseudo-first-order model*:

1qt=????1?????????+1????? (5)

Pseudo-second-order model:

tqt=1????2?????2+????????? (6)

where *k*1 is the pseudo-first-order rate constant (1min-1); *q*t and *q*e are the amounts of dye adsorption at time t and at equilibrium, respectively (mg/g); *k*2 is the rate constant of the pseudo-second-order adsorption (g/ (mg min).

A study of kinetics of adsorption is important as it provides information about the mechanism of adsorption, which is important for the efficiency of the process. The applicability of the pseudo-first order and pseudo-second order model was tested for the sorption of MB dye on adsorbent. The best fit model was selected on the values of correlation coefficient, R2. The investigations of the mechanism of adsorption take place by two kinetic models are pseudo-first-order model, pseudo-second-order model.

The Pseudo First-order Kinetic Model: Fig. 10A shows pseudo- first- order kinetics for adsorption of MB dye adsorption by nanofiber composite. It was noted that in Figure 10A, the experimental qe value (qe = 0.269) doesn't agree with the calculated one (qe = 68.91). This showed that the adsorption of MB dye on the PVA/PEG/GA-MoO3nanofiber composite wasn't a first order kinetic.

The Pseudo Second-Order Kinetic Model: Fig. 10B showed that, there was a good agreement between experimental (qe =0.269) and calculated qe value (qe = 0.269). Table 1 shows comparison of the pseudo first- and second-order adsorption rate constants and calculated and experimental qe value for the used initial dye concentration.

As illustrated in the previous table, the correlation coefficient for the second- order model (R2 = 1) was better than the first-order model (R2 = 0.6). So the experimental kinetic data were further analyzed using pseudo second order.

CONCLUSION

Electrospun PVA/PEG/GA nanofibers have been prepared by electrospinning and crosslinking using GA as the crosslinking agent, The PVA/PEG nanofibers with GA crosslinking showed an excellent mechanical properties, swelling properties and ability to remove of organic dye methylene blue (MB) from water. The crosslinkednano fibers surface was characterized by FTIR, SEM, TGA and confirmed their crosslinking and stability. The introducing of MoO3 nanoparticles to the crosslinkednanofibers surface can significantly increase the adsorption capacity of the composite nanofibers for MB removal. The isotherm studies, Kinetics and thermodynamics were studied to understand the adsorption behavior of PVA/PEG/GA-MoO3 composite nanofibers towards MB. The composite nanofiber mat showed high removal efficiency in aqueous solution for removal of MB and can be used promising adsorbent for dye wastewater treatment.

ACKNOWLEDGEMENTS

This project was supported financially by the Science and Technology Development Fund (STDF), Egypt, under grant no. 15042).

REFERENCES

1. Siddique, M., R. Farooq, A. Khalid, A. Farooq, Q. Mahmood, U. Farooq, A. Raja and S.F. Shaukat, 2009. J. Hazard. Mater, 172: 1007.
2. Wu, X., D. Wu, R. Fu and W. Zeng, 2012. Dyes Pigments, 95: 689.
3. Marin, M.O., V.D. Prete, E.G. Moruno, C.F. Gonzalez, A.M. Garc and V.G. Serrano, 2009. Food Control, 20: 298.
4. Gurusamy, Y.L. Lai and J.F. Lee, 2008. J. Hazard. Mater, 152: 337.
5. Liu, T.H., Y.H. Li, Q.J. Du, J.K. Sun, Y.Q. Jiao and G.M. Yang, 2012 Colloids Surf. B, 90: 197.

6. Jiang, F., Z. Zheng, Z.Y. Xu, S.R. Zheng, Z.B. Guo and L.Q. Chen, 2006. J. Hazard. Mater. B 134: 94.
7. Poznyak, S.K., N.P. Osipovich, A. Shavel, D.V. Talapin, M.Y. Gao, A. Eychmuller and N. Gaponik, 2005. J. Phys. Chem. B, 109: 1094.
8. Ma, P. and R. Zhang, 1999. J. Biomed. Mat. Res., 46: 60.
9. Ondarcuhu, T. and C. Joachim, 1998. Europhys. Lett., 42: 215.
10. Feng, L., S. Li, H. Li, J. Zhai, Y. Song, L. Jang and D. Zhu, 2004. Angew. Chem. Int., 41: 1221.
11. Fong, H. and D.H. Reneker, 2001. In "Electrospinning and formation of nanofibers" in: D.R. Salem (Ed.), Structure Formation in Polymeric Fibers, Hanse, Munich.
12. Liu, Y., R. Wang, H. Ma, B. Hsiao and B. Chu, 2013. Polymer, 54: 2.
13. Bhardwaj, N. and S.C. Kundu, 2010. Biotechnol. Adv., 28: 3.
14. Doh, S.J., C. Kim, S.G. Lee, S.J. Lee and H.J. Kim, Hazard. Mater., 154: 118.
15. Menkhaus, T.J., H. Varadaraju, L. Zhang, S. Schneiderman, S. Bjustrom, L. Liu and H. Fong, 2010. Chem. Commun., 46: 3720.
16. Bjorge, D., N. Daels, S. De Vrieze, P. Dejans, T. Van Camp, W. Audenaert and S.W. Van Hulle, 2009. Desalination, 249: 942.
17. Lin, T., J. Fang, H. Wang, T. Cheng and X. Wang, 2006. Nanotechnology, 17: 15.
18. Tang, C., C.D. Saquing, J.R. Harding and S.A. Khan, 2009. Macromolecules, 43: 2.
19. Destaye, A.G., C.K. Lin and C.K. Lee, 2013. ACS appl mater Inter, 5: 11.
20. Cetiner, S., F. Kalaoglu, H. Karakas and A.S. Sarac, 2010. Text Res. J., pp: 80.
21. Gohil, J.M., A. Bhattacharya and P. Ray, 2006. J. Polym Res., 13(2): 161-169.
22. Lee, K.H., H.Y. Kim, Y.J. Ryu, K.W. Kim and S.W. Choi, 2006. J. Polym. Sci. Pol Phys, 41: 11.
23. Ma, Z., J. Gao, Y. Huai, J. Guo, Z. Deng and J. Suo, 2008. J. Sol-gel Scitechn, 48: 3.
24. Wang, J., H.B. Yao, D. He, C.L. Zhang and S.H. Yu, 2011. ACS Appl. Mater Inter, 4: 4.
25. Fang, X., H. Ma, S. Xiao, M. Shen, R. Guo, X. Cao and X. Shi, 2011. J. Mater Chem., 21: 12.
26. Buell, S., G.C. Rutledge and K.J. Vliet, 2010. ACS Appl Mater Inter, 2: 4.
27. Wang, Y., Y. Zhu, Z. Xing and Y. Qian, 2013. Int. J. Electrochem. Sci., 8: 9851.
28. Ibrahem, M.A., F.Y. Wu, D.A. Mengistie, C.S. Chang, L.J. Li and C.W. Chu, 2014. Nanoscale, 6: 5484.
29. Noerochim, L., J.Z. Wang, D. Wexler, Z. Chao and H.K. Liu, 2013. J. Pow Sour, 228: 198.
30. Manivel, A., G.J. Lee, C.Y. Chen, J.H. Chen, S.H. Ma, T.L. Horng and J. Wu, 2015. Mater Res Bull, 62, 184.
31. Thomas, J.D., M. Marcolongo and A. Lowman, 2003. J. Biomed Mater Res., A. 15: 4.
32. Mansur, H.S., R.L. Oréfice and A.A. Mansur, 2004. Polymer, 45: 21.
33. Chen, N.X. and J.H. Zhang, 2010. Chinese J. Polym. Sci., 28, 6.
34. Sibold, N., C. Dufour, F. Gourbilleau, M. N. Metzner, C. Lagrève, L. Le Pluart and T.N. Pham, 2007. Appl. Clay. Sci., 38: 1.
35. Aytimur, A., S. Koçyiğit, İ. Uslu and F. Gökmeşe, 2015. Int J. Polym. Mater Po, 64: 3.
36. Inbaraj, B.S., K. Selvarani and N. Sulochana, 2002. JSIR, 61: 971.
37. Rubavathi, S.R., A . Rosario, B. Subramanium and A. Jeya Rajendran, 2016. IJIRST, 3(3): 2349.
38. Aksu, Z. and S. Tezer, 2006. Process Biochem., 36: 431.
39. He, X., K.B. Male, P.N. Nesterenko, D. Brabazon, B. Paull and J.H. Luong, 2013. ACS Appl. Mater. Interfaces, 5(17): 8796.